Cerebral Cortex February 2010;20:411–424
doi:10.1093/cercor/bhp112
Advance Access publication June 5, 2009

Human V6: The Medial Motion Area

S. Pitzalis[1,2], M.I. Sereno[3,4,5], G. Committeri[6], P. Fattori[7], G. Galati[2,8], F. Patria[2] and C. Galletti[7]

[1]Department of Education in Sport and Human Movement, University of Rome "Foro Italico," 00194 Rome, Italy, [2]NeuroImaging Laboratory and Laboratory of Neuropsychology, Santa Lucia Foundation, 00179 Rome, Italy, [3]Department of Cognitive Science, University of California, San Diego, CA 92093, USA, [4]Department of Psychology, University College London, London WC1E 7HX, UK, [5]Department of Psychology, Birkbeck College, University of London, London WC1H 0AP, UK, [6]Department of Clinical Sciences and Bioimaging, and ITAB, University Gabriele d'Annunzio, 66013 Chieti, Italy, [7]Department of Human and General Physiology, University of Bologna, 40126 Bologna, Italy and [8]Department of Psychology, Sapienza University, 00185 Rome, Italy

Cortical-surface-based functional Magnetic Resonance Imaging mapping techniques and wide-field retinotopic stimulation were used to verify the presence of pattern motion sensitivity in human area V6. Area V6 is highly selective for coherently moving fields of dots, both at individual and group levels and even with a visual stimulus of standard size. This stimulus is a functional localizer for V6.The wide retinotopic stimuli used here also revealed a retinotopic map in the middle temporal cortex (area MT/V5) surrounded by several polar-angle maps that resemble the mosaic of small areas found around macaque MT/V5. Our results suggest that the MT complex (MT+) may be specialized for the analysis of motion signals, whereas area V6 may be more involved in distinguishing object and self-motion.

Keywords: flowfields, functional localizer, MT/V5, parieto-occipital cortex, wide-field retinotopic mapping

Introduction

Many comparative studies of humans and macaque monkeys have been performed in the visual system, and a number of visual areas have been named in humans based on similarities with nonhuman primate areas (for review, see Sereno 1998; Sereno and Tootell 2005). We recently added area V6 (Pitzalis et al. 2006) to the list of possible human homologues of macaque visual areas (V1, V2, V3, VP, V3A, V4v, and middle temporal MT/V5). Human V6, like macaque V6, is located in the parieto-occipital sulcus (POS) and represents the entire contralateral hemifield (Pitzalis et al. 2006). V6 is characterized by a medially located "upper" field representation distinct from the upper-field representation in lateral area V3A. Human V6, like macaque V6 and owl monkey area M, represents the fovea but emphasizes the visual periphery (Allman and Kaas 1976; Galletti et al. 1999; Pitzalis et al. 2006).

Macaque V6 neurons are very sensitive to moving luminance borders (see Fig. 1), are both orientation and direction selective, and respond well to stimuli of low spatial frequency (see Fig. 1*B*; Galletti et al. 1996, 1999, 2001).

Several neuroimaging studies in humans have shown that medial parieto-occipital cortex is activated by tasks involving visual motion perception (e.g., Cheng et al. 1995; Brandt et al. 1998; Galati et al. 1999; Sereno et al. 2001; Kleinschmidt et al. 2002; Kovács et al. 2008). But none of these studies directly related the activated region to retinotopically organized area V6.

We sought to test whether human V6 is motion sensitive like macaque V6 and to identify a visual stimulus for localizing this area in functional Magnetic Resonance Imaging (fMRI) studies.

We first mapped the retinotopic organization of human V6 as described in Pitzalis et al. (2006). We then studied its functional response profile using motion stimuli (including stimuli similar to those that were effective in activating cells in macaque area V6) as well as flickering stimulation like that previously used in experiments on the human V6-complex (Portin et al. 1999; Portin and Hari 1999; Dechent and Frahm 2003).

We showed that human V6 is a motion area (as evidenced by the fact that it is activated by moving stimuli but not by the same stimuli when they are motionless) providing additional evidence for a homology with macaque V6. Human V6 is also sensitive to flickering stimulation and showed a high selectivity for coherent Flow Field motion, a stimulus not previously tested in macaque V6. Flow Fields selectively activated V6 even when standard sized stimuli were used, making it an excellent human V6 localizer.

Materials and Methods

Subjects

Twenty-three experienced subjects (normal or corrected-to-normal vision) participated in this study (13 women, mean age: 26 years, range: 20–32). Participants gave written informed consent prior to scans (1–5 sessions each) and procedures were approved by local Ethics and Human Subjects Committees. Both block sequence and phase-encoded experimental designs were used. Nine subjects participated in block-design experiments only, whereas 14 subjects participated in both phase-encoded and block-design experiments. Before scanning, subjects were allowed, if they desired, to consume caffeinated beverages to better maintain alertness during the scan session.

Visual Stimuli

Retinotopic Mapping

We mapped polar angle (measured from the contralateral horizontal meridian around the center of gaze) and eccentricity (distance from the center of gaze) using the same phase-encoded retinotopic stimuli previously used to map the visuotopic organization of human area V6 (Pitzalis et al. 2006). High-contrast light and dark colored checks counterphase flickered in either a ray- or a ring-shaped configuration (polar angle and eccentricity, respectively). The average luminance of the stimuli was 105 cd/m^2. Each subject was presented with periodic stimuli (64 s/cycle, 8 cycles/scan), varying in eccentricity or polar angle, in at least 2 pairs of scans. Stimuli moved slowly and

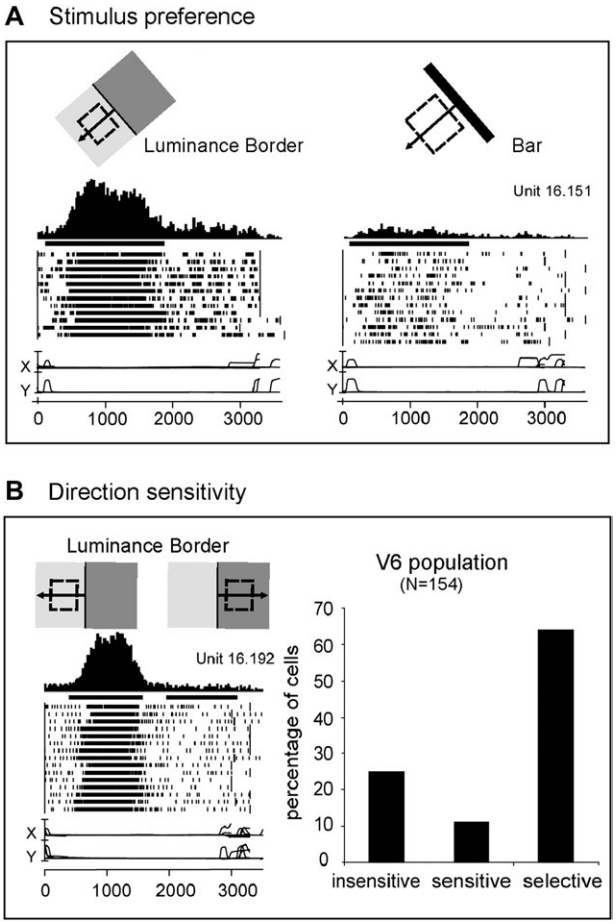

Figure 1. Visual motion sensitivity in monkey area V6. (*A*) V6 neuron better activated by the motion of a Luminance Border (left) than by a bar of the same orientation and direction of motion (right). Each inset contains, from top to bottom: schematic representation of the receptive field (dashed line) and of the stimulus moved across it in the direction indicated by the arrow, peri-event time histogram, bar indicating the duration of visual stimulation, raster plots of spikes recorded during each trial, recordings of horizontal and vertical components of eye positions. Bin width = 20 ms; Eye traces: scale bar, 60 deg. (*B*) "Left": direction selective V6 neuron. All conventions as in (*A*). "Right": Incidence of direction sensitivity in V6 neuronal population. Insensitive: cells whose responses to the stimulus moving in the direction opposite to the preferred one were >80% of the discharge evoked when the stimulus moved in the preferred direction. Sensitive: cells whose responses in the opposite direction were between 20% and 80% of those in the preferred direction. Selective: cells whose responses in the opposite direction were <20% of that in the preferred one.

continuously, and checks reversed between bright and dark at a rate of 8 Hz. Subjects viewed polar-angle stimuli moving in both clockwise and counterclockwise directions in separate sessions. Stimuli were adjusted to respect the distinctive characteristics of macaque V6 as described elsewhere (Pitzalis et al. 2006). We used 1) thin retinotopic stimuli (10 deg in polar angle), 2) a linear scaling in eccentricity (ring stimulus expanding at a constant speed of about 1 deg/s), and 3) a wide-field stimulation (up to 110 deg in total visual extent—see Experimental Setup).

Functional Mapping

In a second set of experiments, we used 4 additional 2-condition stimuli (8 32-s ON, 32-s OFF epochs) described below.

"Low-Contrast Drifting Luminance Edges," hereafter called "Drifting Edges" (see Fig. 2*A*). The stimulus (code by G. Galati) consisted of low-contrast moving luminance edges (ON period) compared with stationary edges (OFF period). In the ON phase, the stimulus moved across the visual field in 1 of 8 directions at 1 of 3 different speeds (19, 30, and 50 deg/s). At the end of each 2- to 5-s sweep, the stimulus changed direction and speed and the luminance contrast phase reversed. OFF blocks consisted of static luminance edges changed every 4 s located at 1 of 16 different spatial positions (1/6, 2/6, 4/6, and 5/6 of the distance along the horizontal, vertical, and diagonal axes, i.e., omitting borders crossing the fixation point) and 2 possible luminance phases (32 stimuli, fairly shuffled). The luminance contrast was low (~5% contrast). The average luminance of the stimulus was 60 cd/m^2.

"Low Contrast Expanding and Contracting rings" hereafter called "Radial Rings" (Fig. 2*B*). Stimuli produced by an X11/OpenGL program (original GL code by A. Dale, ported and extended by M. Sereno) were concentric thin light gray rings (0.2 cycles/deg, duty cycle = 0.2) on a slightly darker-gray background, either moving (7 deg/s—ON period) or stationary (OFF period). During the ON block, the concentric rings periodically contracted and expanded (1 s, 1 s) to avoid generating motion aftereffects during the OFF block. The stimulus luminance contrast was low (~1.5%) as described in Tootell et al. (1995) to better isolate MT+. The average luminance of the stimulus was 61 cd/m^2. Subjects reported after the session that the stimulus produced no illusory perception of self-motion (vection).

"High-contrast Flow Fields" hereafter called "Flow Fields" (see Fig. 2*C*). The same X11/OpenGL software (Dale and Sereno) produced 16-s blocks of coherent dot field motion contrasted with scrambled motion. A new field of white dots was generated every 500 ms (dot size 0.4 × 0.4 deg^2). Dots immediately began to move along a trajectory so as to generate a coherent movement on a plane. The pattern motion was chosen randomly for that 500-ms period from a continuum ranging from dilation to outward spiral, to rotation, to inward spiral, to contraction. The center of the movement was jittered from flow to flow, and the speed varied within a small range. During the scrambled OFF period, dots and their movement vectors were generated as during the coherent ON periods except that each dot trajectory was rotated by a random angle around the pattern center before execution. This scrambled the coherency of movement (at a given point, dots moved in different directions) but preserved the speed gradient (central dots still moved slower than peripheral dots). The average luminance of the stimulus was 31 cd/m^2. This stimulus is freely available for different platforms (IRIX, Linux and Mac OS X—contact sereno@cogsci.ucsd.edu). Both the wide field and regular versions of the optic flow stimulus induced vection according to subject verbal reports after the session. Induced vection was particularly compelling with wide-field stimuli.

"High-contrast Flickering Circle," hereafter called "Flickering" (see Fig. 2*D*). Here, we tested whether area V6 responded to high-contrast (100% luminance contrast) 5-Hz luminance flicker with square contrast modulation in time (code by G. Galati). The average luminance of the stimulus was 45 cd/m^2. During the ON phase, a high-contrast flickered stimulus was presented either in central (20-deg outer radius; Fig. 2*D*, left column) or peripheral (25-deg inner radius; 45-deg outer radius; Fig. 2*D*, right column) positions. The OFF phase was a uniform gray field. The central and peripheral versions of the luminance flicker were tested in separate sessions. They were intended to stimulate the central and peripheral halves of V6.

Experimental Setup

Wide-field stimulation (as described in Pitzalis et al. 2006) was used for all experiments. Stimuli were projected onto a back-projection screen that was viewed directly (not via a mirror). The screen was placed only 10–12 cm from the subject so that visual stimuli subtended up to 100 deg (±50) horizontally, 80 deg (±40) vertically, and 110 deg (±55) in an oblique direction in the visual field. Besides better revealing areas that emphasize the periphery, the wide-field retinotopic stimuli also help avoid a confound in fMRI mapping studies due to surround inhibition (Brewer et al. 2002). As explained previously (Sereno and Tootell 2005; Pitzalis et al. 2006), retinotopic cortical regions having representations of visual space just beyond the peripheral edge of a rotating wedge can generate a periodic signal with a misleading 180-deg phase offset. By stimulating most of the visual field, this beyond-the-stimulus-edge phase inversion is greatly reduced.

All functional experiments used passive viewing and continuous central fixation throughout the period of scan acquisition. Head motion

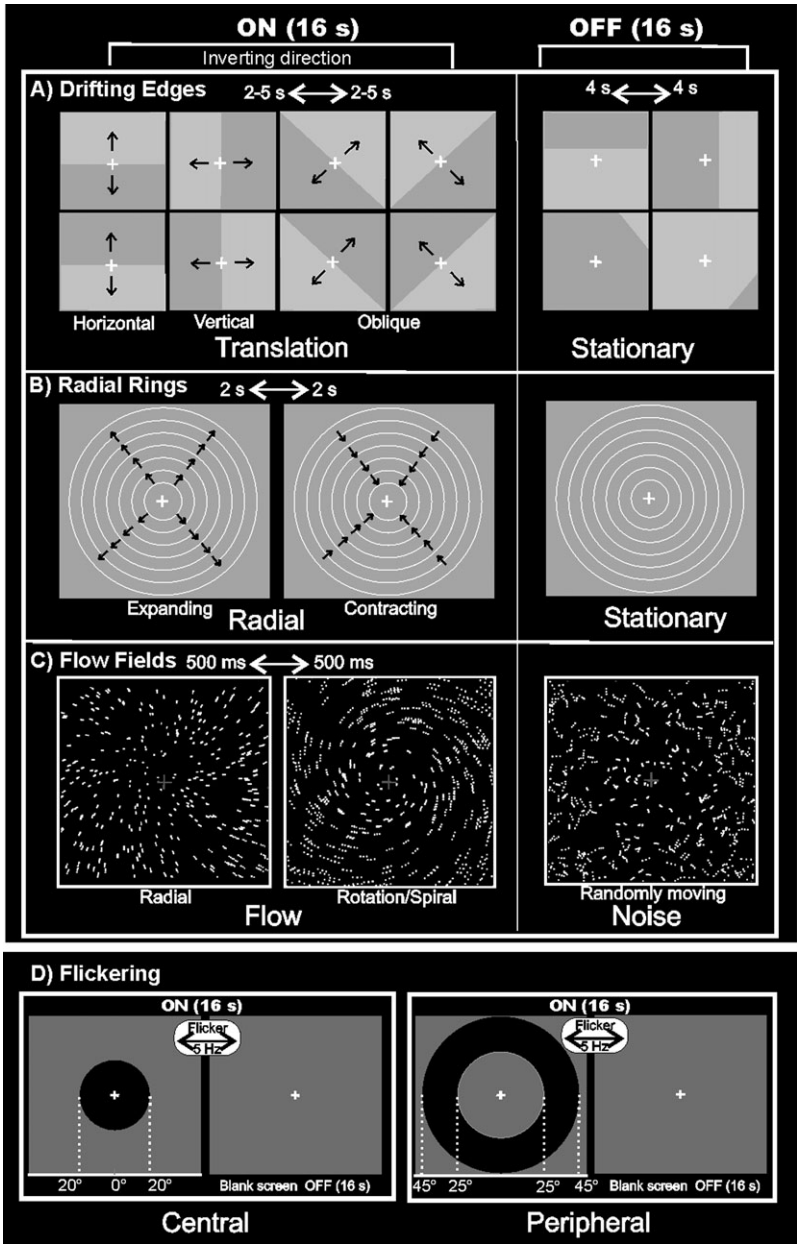

Figure 2. Stimuli used for visual stimulation. (*A*) Drifting Edges. For the ON phase, the edge is shown in the central position of the screen and indicates the 8 possible directions of stimulus motion: vertically (top > down; bottom > up), horizontally (left > right; right > left), and in 2 oblique directions (45 > 225-deg corner and vice versa; 315 > 135-deg corner and vice versa). The directions switched every 2-5 s. The frames of the OFF phase show 4 of 32 possible static frames (16 light/dark and 16 dark/light) located in 4 of 16 spatial positions of the stimulus. (*B*) Radial Rings. The 2 frames of the ON phase show the 2 directions of the radial motion (outward and inward) that switched every 2 s and that were compared with stationary rings presented during the OFF phase. (*C*) Flow Fields. The 2 frames of the ON phase show the 2 different types of coherent motion (radial and rotation–spiral motion) that switched almost every 500 ms and were compared with random motion presented during the OFF phase. For both radial and spiral motions, we tested both expansion and contraction components. (*D*) Flickering. During the ON phase, the high-contrast circles flickering at 5 Hz (100% luminance contrast) were presented either in central (20-deg outer radius; left column) or peripheral (25-deg inner radius; 45-deg outer radius; right column) position. Central and peripheral versions of the luminance flicker were tested in separate sessions. The OFF phase was constituted by a uniform gray field. For all stimuli, we used a wide-field stimulation (up to 110 deg) and the subjects were instructed to fixate the central red cross to minimize eye movements. See Materials and Methods for further details.

was minimized by using a bite bar with an individually molded dental impression mounted on a 6-degrees-of-freedom locking plexiglas arm (Sereno et al. 2001). Subjects were instructed not to forcibly bite the impression but rather to use it as a reference. Subjects' heads were also stabilized with foam pads, and allowed to settle for a few minutes before the bite-bar arm was fixed in position. Interior surfaces were covered with black velvet to eliminate reflections. Visual stimuli were projected using an XGA video projector (1024 × 768, 60 Hz, 10–15 pixels per degree of visual angle) whose standard lens had been replaced with a 7.38–12.3″ focal length XtraBright Zoom lens (Buhl Optical, USA) in order to achieve small high-resolution images on a screen inside the bore (at a distance of 3–4 m).

Imaging Parameters

The magnetic resonance (MR) examinations were conducted at the Santa Lucia Foundation (Rome, Italy) on both a 1.5 T (Siemens Vision, Siemens Medical Systems, Erlangen) and a 3T (Siemens Allegra, Siemens Medical Systems, Erlangen) MR scanner. Single-shot echo-planar imaging (EPI) images were collected using a Small Flex quadrature

surface RF coil placed over occipital and parietal areas (Siemens Vision) and a transmit–receive birdcage head coil (Siemens Allegra). MR slices were 2.5–4 mm thick, with an in-plane resolution of 3 × 3 mm, oriented approximately parallel to the calcarine fissure. Each scan took either 256 s (2-condition experiments) or 512 s (retinotopy), with 128 or 256 single-shot EPI images per slice, respectively (1.5 T: 16–32 contiguous slices with time repetition (TR) = 2000 or 4000 ms, respectively; time echo (TE) = 42, flip angle = 90, 64 × 64 matrix, bandwidth = 926 Hz/pixel; 3 T: 30 contiguous slices with TR = 2000 ms, TE = 30 ms, flip angle = 70 deg, 64 × 64 matrix, bandwidth = 2298 Hz/pixel). The first 8 s of each acquisition were discarded from data analysis. A total of 176 functional scans were carried out on the 23 subjects (56 scans to map retinotopy, and 120 scans for functional experiments).

The cortical surface of each subject was reconstructed from a pair of structural scans (T1-weighted MP-RAGE (magnetization prepared rapid gradient echo), 1 × 1 × 1 mm; 1.5 T: 220 contiguous coronal slices, TR = 11.4 ms, TE = 4.4 ms, flip angle = 108; 3 T: 176 contiguous sagittal slices, TR = 2.00 s, TE = 4.38 ms, flip angle = 8 deg) taken in a separate session using a head coil. The last scan of each functional session was an alignment scan (also MP-RAGE, 1 × 1 × 1 mm) acquired with the surface coil (1.5 T) or head coil (3 T) in the plane of the functional scans. The alignment scan was used to establish an initial registration of the functional data with the surface. Additional affine transformations that included a small amount of shear were then applied to the functional scans for each subject using blink comparison with the structural images to achieve an exact overlay of the functional data onto each cortical surface.

Data Analysis

Anatomical Image Processing

FreeSurfer was used for surface reconstruction (Dale et al. 1999; Fischl et al. 1999). The 2 high-resolution structural images obtained from each subject were manually registered and averaged. After reconstructing each hemisphere, we completely flattened the inflated occipital lobe after first cutting it off posterior to the Sylvian fissure and making an additional cut along the calcarine fissure. Stereotaxic coordinates were calculated through an automatic nonlinear stereotaxic normalization procedure (Friston et al. 1995), performed using the SPM99 software platform (Wellcome Department of Cognitive Neurology, London, UK), implemented in MATLAB (The MathWorks Inc., Natick, MA, USA). The template image was based on average data provided by the Montreal Neurological Institute (MNI) (Mazziotta et al. 1995).

Functional Image Processing

Processing of functional images was performed using FreeSurfer (Dale et al. 1999; Fischl et al. 1999) and SPM (Wellcome Department of Cognitive Neurology).

FreeSurfer Analysis

Analysis methods for phase-encoded data were similar to previous studies (Sereno et al. 1995; Tootell et al. 1997; Hagler and Sereno 2006; Pitzalis et al. 2006). Briefly, *P* values were estimated on a voxel-by-voxel basis by constructing an *F* ratio between "signal" (response amplitude at stimulus frequency) and "noise" (amplitude at other frequencies excluding second and third harmonics) with degrees of freedom equal to the number of time points. The phase of the signal at the stimulus frequency was used to map retinotopic coordinates (polar angle or eccentricity). In standard block-design analysis, pseudocolor scales are usually used to represent the amplitude of the response (after masking the data with a significance threshold). In mapping studies, pseudocolor is also used to represent the phase of the response. In order to concentrate the viewer's attention on the phase, we modulated the saturation of the color as a function of the signal amplitude using a sigmoid function. The sigmoid function was arranged so that visibly saturated phase colors begin to emerge from the gray background at a threshold of $P < 10^{-2}$. The data at most activated cortical surface points have much higher significance values ($P < 10^{-5}$ to 10^{-10}). This procedure has been used in many previous studies (e.g., Tootell et al. 1997). A similar analysis was used to distinguish between positive and negative going MR fluctuations in the case of 2-condition stimulus comparisons (e.g., MT+ mapping). This analysis assumes that the noise is uncorrelated, an assumption known to be false for fMRI time series (Zarahn et al. 1997). The *P* = values reported should therefore considered to be rough estimates of the levels of statistical significance of the periodic activation. However, the lack of any trace of activation in large stretches of nonretinotopic visual areas in inferotemporal and inferior parietal cortices suggests that this threshold is not too permissive.

The boundaries of retinotopic cortical areas (V1, V2, V3, VP, V3A, and V4v) were defined on the cortical surface for each individual subject on the basis of phase-encoded retinotopy (DeYoe et al. 1994, 1996; Engel et al. 1994, 1997; Sereno et al. 1995) and subsequent calculation of visual field sign, which provides an objective means of drawing borders between areas based on the angle between the gradients (directions of fastest rate of change) in the polar angle and eccentricity with respect to cortical position (Sereno et al. 1994, 1995). The visual field sign indicates whether each small patch of cortex represents the visual field as a mirror-image or a non–mirror image. As in nonhuman primates, early cortical areas (e.g., V1) are characterized by one visual field sign (e.g., mirror image). Adjacent areas often have opposite visual field sign. Each field sign map shown here was based on at least 4 scans (2 scans for polar angle and 2 scans for eccentricity). The visual field sign method is merely a generalization of the notion that border between areas are often defined by meridians (but occasionally by other lines in the visual field) with duplicated representations of visual space on either side of the meridian (or other line). Although a series of color maps with superimposed isophase contour lines contain no more information than a single color map, the sequence makes the duplicated fields easier to see because small but significant variations in phase are difficult to represent using hue alone (see, e.g., Hadjikhani et al. 1998; Pitzalis et al. 2006). Such a series can also be thought of as the time sequence of activations for one stimulus cycle (though the width of the activated band of cortex at one point in time varies as a function of receptive field size and other factors).

The phase of the periodic response is delayed because of a finite vascular response time. Also, it is possibly differently delayed in different areas. In our stimuli, the basic stimulus frequency was low enough so that the hemodynamic delay was much smaller than one cycle, eliminating whole-cycle phase ambiguity. Data from a reversed-direction stimulus can be used to verify a map; but reversed data can also be combined with unreversed data to correct residual phase delay differences between areas (Sereno et al. 1995; Hagler and Sereno 2006). In the 3-T data, we calculated the vector average at each voxel of the response amplitude and phase angle obtained for opposite directions of stimulus motion (clockwise vs. counterclockwise) after reversing the sign of the phase angle for one direction. This procedure reduced noise in both visual and nonvisual cortical areas because the vector sum operation strongly penalizes voxels with inconsistent phase in opposite directions, even if they are separately significant.

SPM Analysis

In data analyses performed with SPM99 (Wellcome Department of Cognitive Neurology) functional images from each participant were coaligned with the high-resolution anatomical scan (MP-RAGE) taken in the same session. Images were motion corrected, transformed into MNI space (Mazziotta et al. 1995) using a nonlinear stereotaxic normalization procedure (Friston et al. 1995), and smoothed with a 3D Gaussian filter (6-mm full-width-half-maximum). For the 4-block sequence experiments, a standard group analysis was performed according to a general linear model, modeling "ON" blocks as box-car functions convolved with a canonical hemodynamic response function. Significance was judged at the voxel level and by cluster size. Correction for multiple comparisons was performed using distribution approximations from the theory of gaussian fields (Worsley et al. 1992) at the cluster level ($P \leq 0.01$ corrected), after forming clusters of adjacent voxels surviving a threshold of $P \leq 0.01$ uncorrected (Friston et al. 1996). Data from Flickering experiment were processed using 2 types of analysis strategies. First, in a direct approach designed to map the cortical representation of stimulus features, the central and peripheral flickering stimuli were separately contrasted with a blank field. Second, in a differential approach, the peripheral flickering stimulus followed by a blank field was contrasted with the central flickering stimulus again followed by

a blank field. Localization and visualization of individual activations by SPM were achieved by using BrainShow, in-house software (code by G. Galati) for visualization of fMRI data. This Matlab-based Analyze-SPM image viewer allows superimposition of individual SPM maps on individual brain slices or folded, inflated, and flattened representations of cortical surfaces reconstructed by FreeSurfer. We also used it to superimpose SPM group maps (in MNI space, see above) on the cortical surface of the single-subject MNI canonical brain (Colin27), whose cortical surface was reconstructed using FreeSurfer.

Results

Retinotopic Mapping

A wide-field retinotopic experiment was carried out for each single subject to individually define the shape and position of area V6, as described in Pitzalis et al. (2006). Figure 3*A* shows a color plot of the response to the rotating wedge stimulus, displayed on the flattened cortical surface representation from the left hemisphere of one participant (see caption of Fig. 3 for further details). Wide-field stimuli visualized a continuous mosaic of retinotopic maps in the occipito-temporal region, progressing from V3A/V7 (Tootell et al. 1997, 1998) to lateral occipital cortex (in line with recent reports, e.g., Larsson and Heeger 2006), up to temporal regions between the inferior and superior (STS) temporal sulci. Wide-field stimuli were especially more effective than standard stimuli for retinotopically mapping parietal and middle temporal areas (which remain silent or less activated when stimulated with visual stimuli of standard size).

Figure 3*B* shows the details of the polar-angle representation in a series of 8 close-ups of the flattened surface taken from left lateral middle temporal cortex (white box) of the same subject. The splitting of phase contours illustrated in phase movie (3*B*) more clearly marks the position of vertical and horizontal meridians. In Pitzalis et al. (2006), the borders of human V6 were defined by 2 vertical meridians, a medial 1 superior and anterior to peripheral lower field V2/V3 (middle of the red spot) and a lateral 1 superior to V3A (middle of the green spot). The phase movie in middle temporal cortex reveals the presence of additional well-defined retinotopic maps (indicated by white outlines in the first frame of the movie in Fig. 3*B*). Among these maps, the middle region (with an anterior facing upper field) contains a complete representation of the contralateral visual field (see also Fig. 3*C* showing polar-angle maps in 4 additional hemispheres). We identified this area as MT/V5 in light of primate visuotopic organization based on neurophysiological data (e.g., Allman and Kaas 1971; Zeki 1974; Gattass and Gross 1981; Van Essen et al. 1981) and previous fMRI data in this region (e.g., Huk et al. 2002; Wandell et al. 2005; Smith et al. 2006). The location and extent of area MT/V5 are indicated with a white outline in both the flattened surface (3*A*) and the first frame of the movie (3*B*) as well as in the 4 panels of Figure 3*C*. Note that the upper visual field

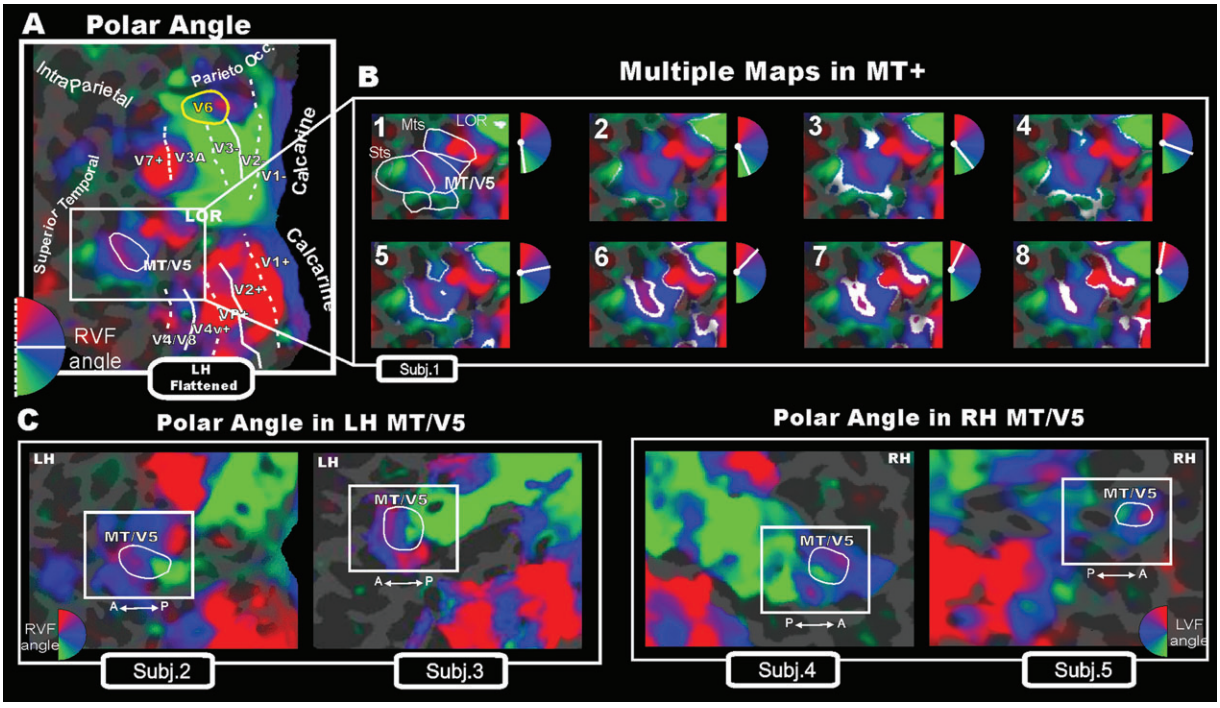

Figure 3. Wide-field retinotopy of polar-angle representation. Color hue indicates the response phase, which is proportional to the polar angle of the local visual field representation: Green/blue/red areas represent lower/horizontal/upper fields, respectively (see hemifield icons). (*A*) Flattened reconstruction of the left hemisphere of one participant (as reported in Pitzalis et al. 2006) showing retinotopic phase–encoded signal in the dorsal and ventral cortical areas (including medial V6 and lateral MT/V5). Here and in the following figures reporting individual data, the flat map also shows the boundaries of the early visual areas and of area V6 defined by mapping visual field sign (Sereno et al. 1994, 1995). Dotted and solid white lines reported on the flat maps indicate vertical and horizontal meridians, respectively, and yellow outlines indicate location and borders of the human area V6. Major sulci (dark gray) are labeled as follows: Parieto-occ, parieto-occipital sulcus; Intraparietal sulcus, STs, Superior Temporal sulcus; MTs, Middle Temporal sulcus. LOR, Lateral Occipital Region. (*B*) Detailed organization of the polar-angle representation shown using close-up views of the flattened left lateral middle temporal (white box) regions of the same subject. In each frame, response-phase contours are marked with white stripes representing the cortical regions activated by a single polar angle and indicated in white in the small hemifield icons located at the upper right of each snapshot. The complete range of phases in one hemifield (180 deg) is illustrated across the 8 close-ups of the flattened surface. (*C*) Retinotopy of polar-angle representation in MT/V5 area (white outline) shown in other 2 left (left part) and 2 right (right part) hemispheres using close-up views of the flattened lateral middle temporal (white box) regions.

representation (red spot) does not belong entirely to area MT/V5 (3*A*–*B*–*C*). The doubling of the phase contour indicates that there is a second representation of the upper visual field outside and anterior to area MT/V5, possibly corresponding to part of the upper-field representation of the "middle temporal crescent" (area MTc) in New World primates (Kaas and Morel 1993; Rosa and Elston 1998). The lower field representation outside and posterior to MT might be the lower VF representation of MTc (called area V4T in the macaque; Desimone and Ungerleider 1986; Gattass et al. 1988).

Responses to Visual Motion

We first tested the sensitivity of human area V6 to translational motion using a visual stimulus similar to that used in Galletti's lab to map the macaque V6 during single-unit experiments. Because cells in macaque V6 are strongly activated by moving luminance Borders (Fig. 1; see also Galletti et al. 1996), we expected high fMRI activity in the human V6 for this stimulus. There are no previous fMRI studies using exactly this stimulus. Figure 4 shows the fMRI activations of area V6 for these unidirectional motion stimuli (Drifting Edges), displayed on flat maps from left and right hemispheres of 3 participants. In this and following figures showing individual data, we also reported the location of the motion-sensitive cortex (MT+; see white boxes) functionally mapped by additional scans as described in the Methods.

Figure 4 shows that Drifting Edges elicited a functional activation in human V6 bilaterally in almost every case. V6 was the most systematically activated area (active in 87% of the

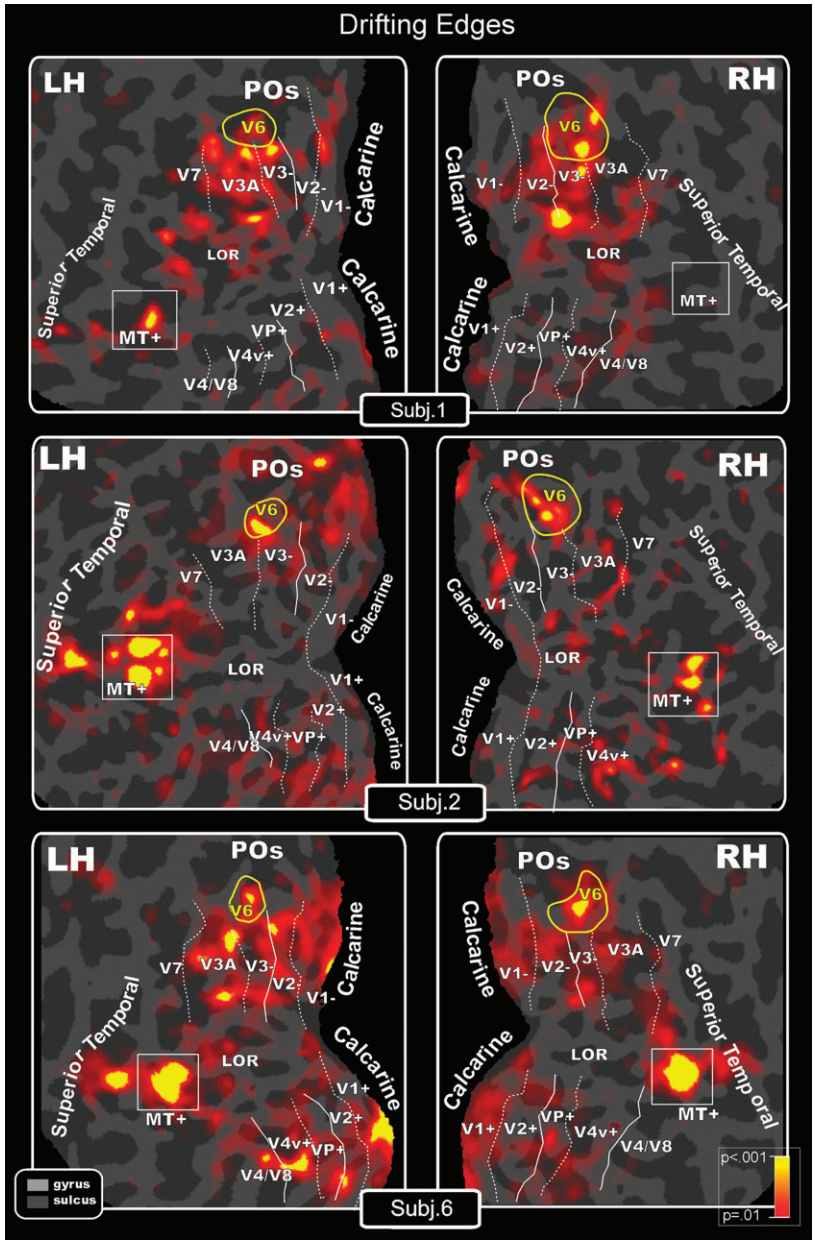

Figure 4. Drifting Edges (both V6 and MT+ response). Topography of motion-selective activity by fMRI mapping from unidirectional motion stimuli displayed on flat maps from left and right hemispheres of 3 participants. Figure shows the differentiated blood oxygen level–dependent (BOLD) activity between conditions: red–yellow regions indicate in a pseudocolor scale higher BOLD activity ($P < 0.001$) during moving than during stationary luminance edges. Main sulci have text labels. POs, Parieto-Occipital sulcus. Other labels and logos are as in Figure 3.

subjects), as expected from single-unit recordings in macaque. This simple unidirectional motion stimulus elicited a functional response in other visual areas, again as expected from single-unit recordings in macaque: in MT+ (61%), STS (58%), and V3/V3A (53%). This stimulus did not activate all of V6 and activated surrounding areas V3 and V3A, too, limiting its value as a localizer.

We also tested the responsiveness of human area V6 to low-contrast radial motion (Radial Rings), the stimulus originally used to functionally map the human motion middle temporal area (Tootell et al. 1995). In macaques, MT/V5 and V6 both contain a high percentage of direction selective cells (Zeki 1974; Maunsell and Van Essen 1983; Desimone and Ungerleider 1986; Galletti et al. 1996), are richly interconnected (Shipp et al. 1998; Galletti et al. 2001), and both receive directly from the layer IVB of the primary visual cortex (Shipp and Zeki 1989; Galletti et al. 2001). Hence, although it is not proved that MT/V5 and V6 projections originate from the same neurons of layer IVB (see Vogt-Weisenhorn et al. 1995), one might have expected that human area V6 would be driven by stimuli activating human MT+. Previous data reported in the literature (e.g., Zeki et al. 1991; Watson et al. 1993; Dupont et al. 1994; Tootell et al. 1995) emphasized activations in the lateral temporal cortices but not in the parieto-occipital cortex (though see Cheng et al. 1995).

Figure 5 (top row) shows results from Radial Rings motion experiment displayed on flat maps from the left hemispheres of 5 participants. This stimulus strongly activated MT+, as expected (e.g., Tootell et al. 1995), but area V6 was not driven by this contrast. This result is consistent across the subjects illustrated in Figure 5 (5/5 hemispheres) and in almost all tested subjects (V6 was not activated in 93% of subjects). We also found quite consistently (66%) a motion-selective response in the lateral occipital region (LOR) between dorsal V3 and MT+ (see also Smith et al. 1998; Tootell and Hadjikhani 2001; Larsson and Heeger 2006; Georgieva et al. 2008 and Dupont et al. 1997; Van Oostende et al. 1997 on the kinetic occipital region, KO). Systematic (62%) spots of functional activation were also found in the posterior part of V3A (inferior part of V3A in the flattened map), as previously observed by Sereno et al. (2001).

We then tested V6 sensitivity to another type of motion stimulus, Flow Fields, which contrasts coherent optical flow stimulation with a scrambled control (see Materials and Methods). Sereno et al. (2001) showed that Flow Fields activated several posterior areas, including the superior (medial) end of human V3A and a small area medial to it in the POS (see Fig. 4 in Sereno et al. 2001; see also the "VIP/SPO" focus in Tootell et al. 1996, Fig. 2). The activated POS area was located approximately in the same cortical region where V6 is located. To confirm this was the case, we made a direct comparison. Figure 5 (bottom row) shows results from Flow Fields motion experiment displayed on flat maps from the left hemispheres of the same 5 participants reported in the top row of Figure 5. Flow Fields did in fact activate human area V6 in every case illustrated here (5/5 left hemispheres) and in 100% of all subjects. As expected, this wide-field coherent motion activated other motion areas. We found a less consistent (53%) motion-selective response in the anterior part of V3A (superior part in the flattened map), as previously observed by Sereno et al. (2001). In agreement with previous studies using optic flow (e.g., Cheng et al. 1995; Morrone et al. 2000; Smith et al. 2006), we also found a weaker motion-selective response in the superior temporal sulcus, in about one-third of subjects (37%). Activation was also sometimes found (21%) in dorsal visual area

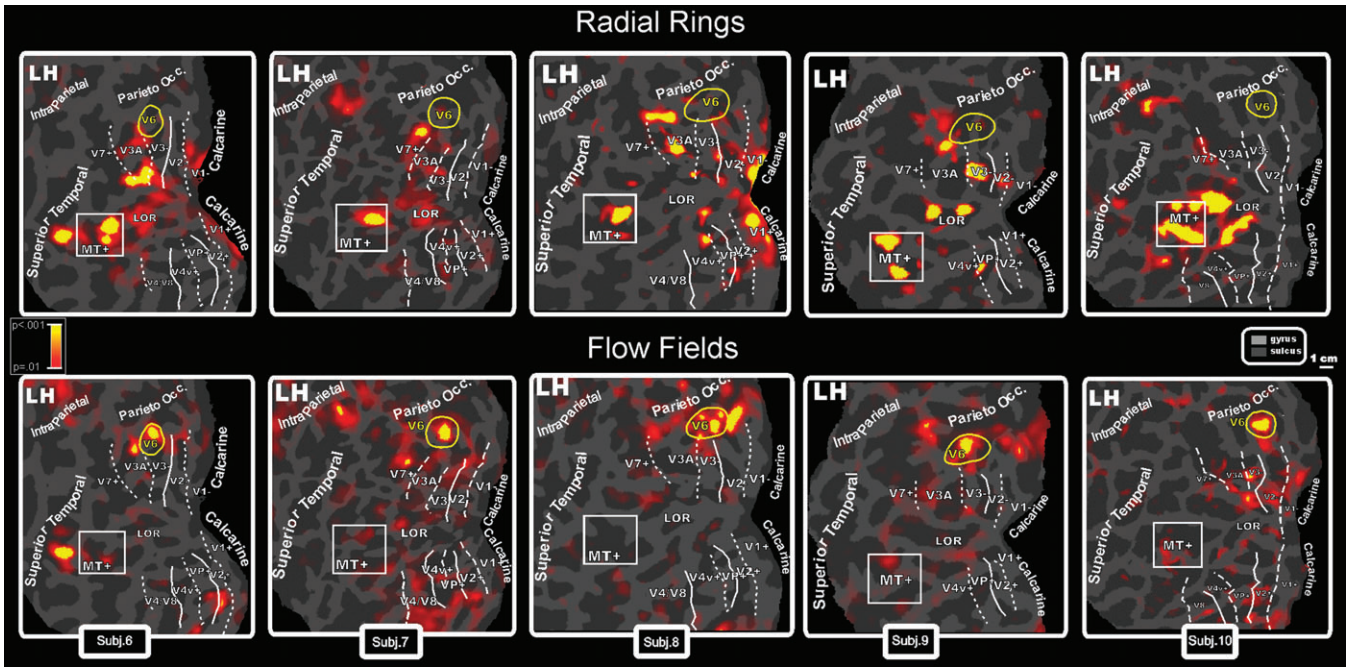

Figure 5. Topography of motion-selective activity by fMRI mapping from Radial Rings (Top: MT+ but not V6 response) and Flow Fields (Bottom: V6 but not MT+ response) stimulations. Results are displayed on flat maps from the left hemispheres of 5 participants. Figure shows the differentiated BOLD activity between ON and OFF conditions. Top row: Red–yellow regions indicate in a pseudocolor scale higher BOLD activity ($P < 0.001$) during radially moving rings than during stationary patterns. Bottom rows: Red–yellow regions indicate higher activity ($P < 0.001$) during rotating and dilating random dot fields than during scrambled moving random dot fields. Main sulci have text label. Other labels and logos are as in Figure 3.

V2 and in a region joining the horizontal and posterior segments of the intraparietal sulcus (IPS, near the location of the original LIP/IPS1 in Sereno et al. 2001), where single units in monkey are reported to be modulated by optic flow stimuli (Siegel and Read 1997). Across all subjects, V6 was the most strongly activated focus.

We never observed an fMRI signal in the motion region MT+ in any of the subjects. This was likely due to the subtraction paradigm we used in the present experiment (coherent motion minus incoherent motion)—MT+ was almost certainly activated by both coherent as well as incoherent movements. A possible explanation is that the transient changes accompanying the onset of a new dot field every 500 ms strongly excite MT cells during both coherent and noise blocks. These responses might mask some selectivity to coherent motion in MT. Note that both Radial Rings and Drifting Edges, by contrast, had a static "OFF" phase.

Some participants were studied with a stimulus of standard size (23 deg × 12 deg) instead of a wide field (100 deg × 80 deg). In Figure 5, the 2 columns to the right show results taken at 3 T using standard size stimuli. The response profiles of the 2 motion-sensitive areas MT+ and V6 were unaffected by the stimulus size. Area V6 (but not MT+) was selectively driven by Flow Fields even with a standard size stimulus. Conversely, MT+ (but not V6) was optimally driven by Radial Rings regardless of stimulus size. The lack of a V6 contralateral response to standard sized retinotopic mapping stimuli is not inconsistent with this result: Standard-sized thin-ray retinotopic mapping stimuli suffer in V6 both because of their inadequate visual field coverage and because they contain only small regions of coherent motion. Coherent versus incoherent Flow Field stimuli can be used as a convenient localizer for V6, even at standard stimulus sizes.

Figure 6 shows high threshold ($P = 10^{-9}$) group-averaged contralateral fMRI activations for Radial Rings and Flow Fields superimposed on the left and right occipital flat maps, as well as on the folded left and right hemispheres of the MNI template (shown in the bottom part of the figure). The complementary pattern of results described in individual subjects is even more evident in the group analysis—V6 was activated by the structured motion stimuli (Flow Fields) but not by the simple radial motion (Radial Rings), whereas the opposite pattern was observed in MT+. The other regions responding to Radial Rings (posterior V3A) and Flow Fields (anterior V3A and STS) only survive at lower thresholds.

The fundus of the POS (dashed lines) is drawn to aid the anatomical location of area V6 in the Figure 6 flat maps. The most dorsal part of the human POS often has a "Y" shape, with anterior and posterior branches dorsally located and variably configured across individuals. As previously demonstrated (Pitzalis et al. 2006), the retinotopic map of V6 is consistently located in or near the posterior branch of the POS, corresponding to the following MNI coordinates ($x = \pm 9$, $y = -82$, and $z = 36$). The posterior branch of the POS can be considered to be the anatomical marker for human V6, as confirmed by Figure 6. Note that human V6 occupies a more superior position than macaque V6 (see Fig. 1 in Pitzalis et al. 2006), which can be explained by considering how V1 has changed with respect to the calcarine in humans, that is, the posterior-around-to-medial movement of human V1 (see Fig. 10, right, in Pitzalis et al. 2006). V6 sits in a more superior position in humans because it

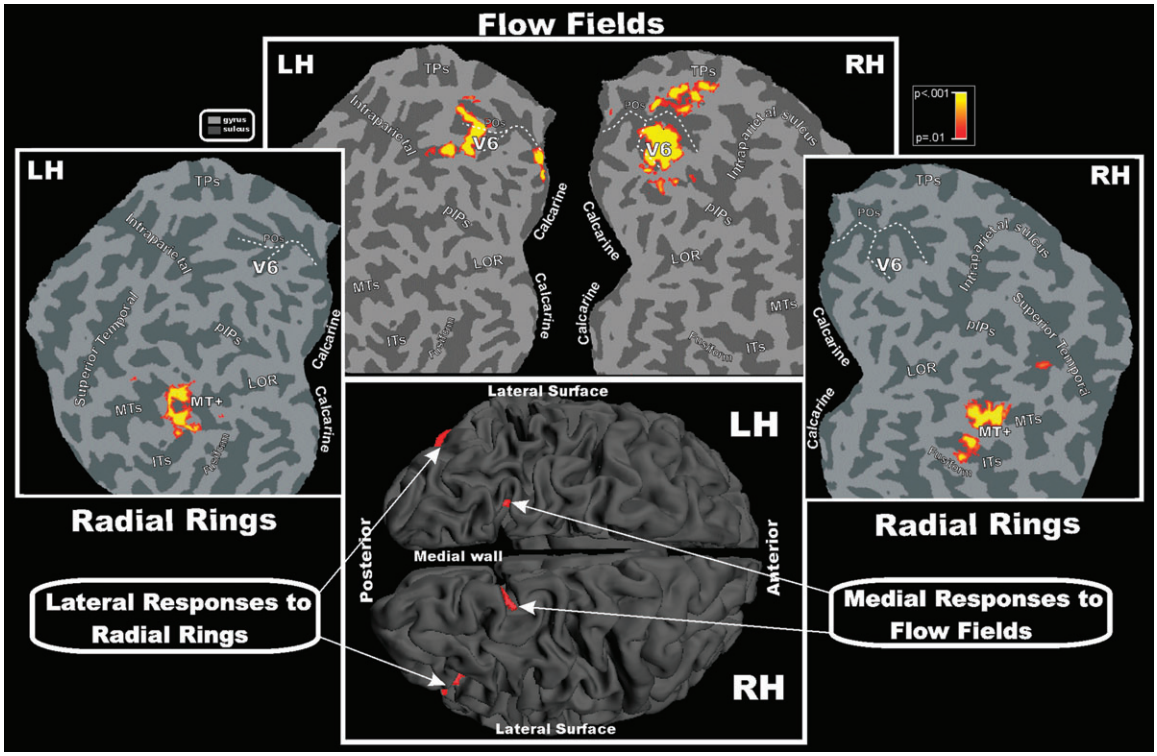

Figure 6. Group contralateral fMRI activations for the Flow Fields and Radial Rings stimuli superimposed on left and right occipital flat maps of the SPM canonical brain in MNI space. The pseudocolor scale in the top right of the figure indicates the statistical significance of the activations. The fundus (dashed lines) of POS is also drawn in both hemispheres to aid comparisons. Major sulci (dark gray) and gyri are labeled as follows: TPs, transverse segment of the parietal sulcus; pIPs, posterior segment of the IPS; MTs, middle temporal sulcus; ITs, inferior temporal sulcus; fusiform, Fusiform gyrus. Bottom: group fMRI activations for the same visual stimuli superimposed on the left and right folded hemispheres (dorsal view) of the SPM canonical brain in MNI space. Other labels and logos are as in Figures 3 and 4.

is no longer overlaid by an occipital operculum and because of peripheral V1/V2 "overflow." Nevertheless, its neighbor relations on the unfolded surface are unchanged.

Responses to Flickering: Center versus Periphery

Because previous neuroimaging studies have demonstrated visual activation along the human POS for flickering stimulations (e.g., Dechent and Frahm 2003; Stenbacka and Vanni 2006), the responsiveness of human area V6 to this type of stimulation was tested in a separate experiment. There are no single-unit data on macaque V6 responses to flickering stimuli. However, Galletti et al. (1991) reported that in some cases, the firing rate changed in accordance with sudden changes in visual background, particularly to switching on and off the background light. Note also that macaque V6 receives direct projections from layer 4B of V1 (Galletti et al. 2001), which in turn receives from the magnocellular-recipient layer 4C-alpha.

The group data reported in the left part of Figure 7 show that flickering stimulations produced widespread activation of dorsal and ventral visual areas that was consistent with their retinotopic organization. fMRI activation was found also in the POS, mainly for peripheral stimulation. The flickering stimulus also evoked responses in and around MT+, in agreement with single-unit data showing that monkey MT/V5 is activated by luminance flicker (Malonek et al. 1994) or flashed stimuli (e.g., Zeki 1980; Albright 1984; Felleman and Kaas 1984; Rodman and Albright 1989; Lagae et al. 1994). In the middle temporal region, a dorso-ventral peripheral-to-central trend mimicked that of monkey middle temporal cortex (Allman and Kaas 1971; Gattass and Gross 1981; Van Essen et al. 1981).

Figure 8 illustrates a single subject. In V1, V2, and V3, the area activated by the central stimulus was slightly larger than the area activated by the (larger) peripheral stimulus. In V6, by contrast, the central stimulus produced a much smaller relative activation, indicating it has a de-emphasis of central fields. These data are consistent with the eccentricity plot shown in Pitzalis et al. (2006). They also resemble what is found in macaque V6 (Galletti et al. 1999) and owl monkey area M (Allman and Kaas 1976), where the representation of the central 20 deg occupies a small lateral part of the area, whereas the medially located periphery is much larger.

The right part of Figure 7 and the right part of left and middle sections show group and individual results, respectively, from the differential approach (contrasts). The results in early

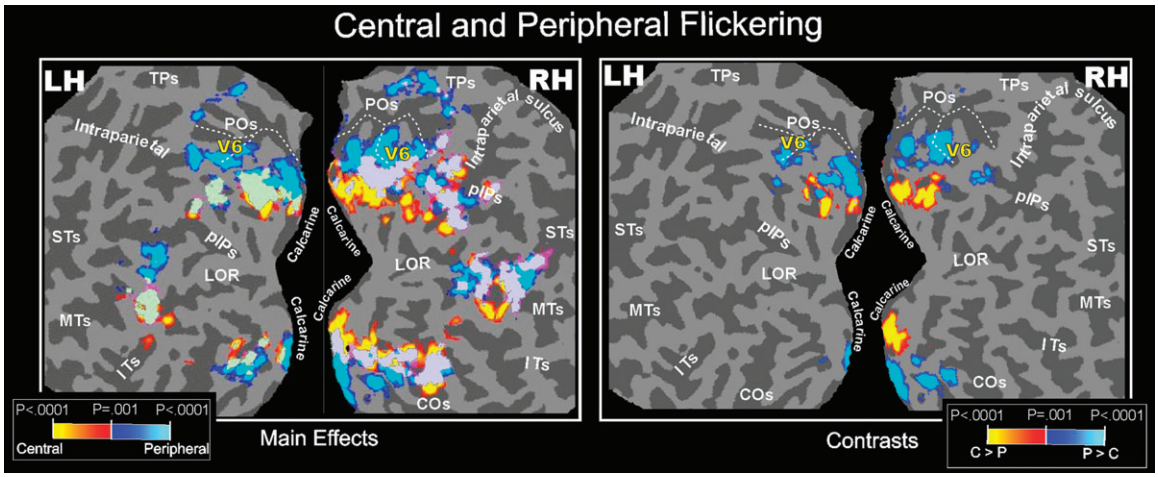

Figure 7. Central and Peripheral Flickering (Group Data). Group fMRI activations from Flickering stimulus, displayed on occipital flat maps of the left and right hemispheres of the SPM canonical brain. Left and right sections of the figure show results from the direct (main effects) and differential (contrasts) approach, respectively. Functional activations from stimuli presented separately in central (0–20 deg) and peripheral (25–45 deg) parts of the visual field are color coded (red and blue, respectively) and are shown together in each flat map (light green, overlap). The fundus (dashed lines) of POS is also drawn in both hemispheres to aid comparisons. The pseudocolor scale in the bottom of both figures indicates the statistical significance of the activations. STs, Superior Temporal sulcus; COs, Collateral Sulcus. Other labels and logos are as in Figures 3, 4, and 6.

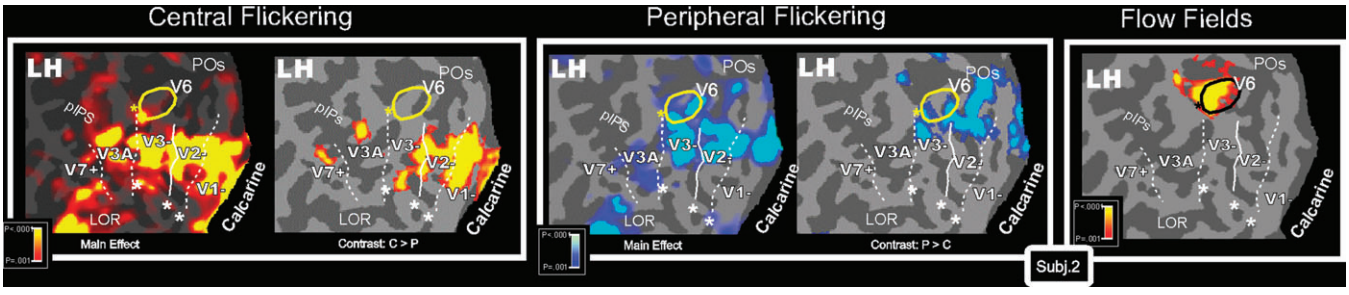

Figure 8. Flickering and Flow Fields (Individual Data). Individual results of one single subject displayed on flat maps from close-ups of the left hemisphere (only the dorsal visual areas are shown). The position and borders of area V6 (as retinotopically defined in this subject) are indicated with a continuous yellow outline, except for the rightmost map where the V6 outline is in black to avoid color masking with the yellow colored fMRI activation spots. The asterisk indicates the representation of the center of gaze as retinotopically mapped. Left and middle sections: fMRI activations for Flickering stimulus from direct (main effects) and differential (contrasts) approach, respectively. Functional activations from stimuli presented separately in central (0–20 deg) and peripheral (25–45 deg) parts of the visual field are color coded (red and blue, respectively) and are shown separately in each flat map. Right section: individual fMRI mapping from Flow Fields stimulus from the same subject as in left and middle sections. Other labels and logos are as in Figures 3, 4, and 6.

areas make sense in light of the main effects described above. Because of increased receptive field size and scatter combined with smaller areal extent in higher cortical visual areas (e.g., MT+, LOR, and IPS), the use of a differential paradigm reduces the overall activation volume there. In V6, the emphasized periphery survived this contrast (unlike the periphery of MT+) but the de-emphasized central visual representation fell below our differential contrast threshold.

In summary, present fMRI data confirm that the POS region (including V6) is activated by flicker, in line with previous neuroimaging studies (e.g., Portin and Hari 1999; Vanni et al. 2001; Dechent and Frahm 2003; Stenbacka and Vanni 2006). However, even with a differential approach, flicker elicits activation that extends beyond the borders of V6 dorsally and ventrally up to the junction between POS and calcarine sulcus. In a previous study, Dechent and Frahm (2003) found a flicker-related cluster of activation in the POS above the junction with the calcarine sulcus. They proposed that this flickering response region was a human homologue of monkey V6/V6A complex. Our combined mapping plus functional data shows, by contrast, that the source of the parieto-occipital luminance response includes not only V6 but also the peripheral parts of the dorsal V2 and V3, and other areas anterior and inferior to V6.

The Flow Fields stimulus is more selective than flicker in isolating V6. Flow Fields selectively activated the whole extent of V6, filling the outline of area V6 drawn from the polar-angle retinotopic map (Fig. 8—all results same subject).

Discussion

Retinotopic mapping and 4 functional experiments were used to verify that human area V6 is a motion-sensitive area and to identify a straightforward functional localizer for routinely outlining this area.

Wide-Field Retinotopic Maps

Wide-field retinotopic mapping revealed that the retinotopic organization and neighbor relations of human V6 closely resemble those reported for macaque V6 (Galletti et al. 1999; Pitzalis et al. 2006). Present results confirm this finding and show that the retinotopic organization of human V6 can also be seen, though less clearly, by comparing the main effects of central and peripheral flickers. However, the V6 central response does not survive a center > periphery contrast, probably because of the combination of large receptive fields, a small overall cortical extent, and a de-emphasized center of gaze (Galletti et al. 1999). Thus, both the central and peripheral stimuli used here activate the central representation of V6 (Fig. 8, left column of left and middle sections), and only the most peripheral part of V6 (>40 deg eccentricity) will survive a center–peripheral comparison (right column of middle section).

Previous magnetoencephalographic (e.g., Portin and Hari, 1999) and fMRI (e.g., Dechent and Frahm, 2003) studies using similar stimuli and approaches failed to reveal a retinotopic organization along the POS. However, this might be due to the relatively small size of the stimuli they used; even their "peripheral" stimulation covered only the central 20 deg of the visual field, which we show here to activate only a small, lateral part of the area (see Fig. 8 left).

The wide-field mapping stimuli used here also resulted in improved maps in the lateral occipital cortex and MT+. In particular, the polar-angle maps confirmed the presence of an anterior facing upper-field representation in MT/V5, in line with previous reports (e.g., Huk et al. 2002) and with data from nonhuman primates (Allman and Kaas 1971; Gattass and Gross 1981). Previous works reported the existence of coarse retinotopic maps within the motion responsive MT+ region (e.g., Huk et al. 2002; Wandell et al. 2005; Smith et al. 2006). The clearer results here may be due to the use of wider field stimuli. We also observed a number of other polar-angle maps around MT/V5 (see Fig. 3), which resemble the mosaic of small areas found around nonhuman primate MT (Gattass and Gross 1981; Van Essen et al. 1981; Desimone and Ungerleider 1986; Sereno et al. 1994). It is now generally acknowledged that the relatively large motion-sensitive region originally labeled V5 (or MT) in humans (Watson et al. 1993; Tootell et al. 1995) is probably a complex of several areas—the "MT complex" or "MT+." The discovery of a mosaic of small retinotopic areas around retinotopic MT/V5 found here nicely fits with this hypothesis.

Future studies using wide-field retinotopy will be needed to better define the retinotopic properties of the mosaic of small areas found around area MT/V5.

Human V6: A Motion Area Highly Sensitive to Flow Fields

Present data reveal that human V6, like macaque V6, is a motion area (Galletti et al. 1996), further strengthening the case for the homology between these cortical areas in humans and macaques. Two of the 3 types of motion stimuli we used activated human V6. The fact that flicker also activates V6 indirectly supports the hypothesis that it is a motion area, as motion-sensitive cells typically respond briskly and transiently to stationary stimuli and are therefore activated by flickering stimulations (e.g., Malonek et al. 1994).

Human V6 responds to unidirectional motion (Drifting Edges) and to the coherent motion of dot fields (Flow Fields). Among these 2 motion stimuli, Flow Fields turned out to be more powerful than Drifting Edges. As luminance borders have been demonstrated to strongly activate single V6 cells in macaque (see Fig. 1; Galletti et al. 1996), the small response in human V6 was unexpected. It might be that, because of the strict direction and orientation selectivity of V6 cells (Galletti et al. 1996), the total number of cells activated by a single moving step in the fMRI experiments is much less than the total number of cells activated by the Flow Field stimulus, where direction and speed of movement, as well as type of movement coherence, changed every 500 ms.

The Flow Fields stimulus used here produces a pattern of coherent motion stimulation similar to the continuously changing optic flow generated when a person moves through in a complex environment (Koenderink 1986). In addition, wide-field Flow Fields were very powerful in inducing a compelling perception of self-motion (vection) and this could be a window into the function of V6. Previous functional imaging studies reported activation in the medial parieto-occipital cortex for coherent wide-field stimuli, such as patterns simulating forward self-motion (e.g., Cheng et al. 1995; Brandt et al. 1998; Galati et al. 1999; Previc et al. 2000; Kleinschmidt et al. 2002; Kovács et al. 2008). As noted by Rosa and Tweedale (2001), human clinical studies have reported that electrical stimulation of the cortex in the expected location of V6 in human POS produces hallucinations of visual motion in the contralateral field (Richer et al. 1991), which included a "transparent circle" moving to the periphery, and sustained motion of objects either toward the periphery or away from the subject (possibly suggesting

contraction), whereas lesions in the human POS (but avoiding MT+) also produced motion related disturbances (Heide et al. 1990; Blanke et al. 2003). Interestingly, epileptic seizures within the precuneus produce linear self-motion perception (Wiest et al. 2004). Given this evidence, V6 may be specialized for the analysis of motion especially in relation to self-movement.

Several previous studies have investigated the neural correlates of optic flow in humans, but none of them looked at area V6 and have instead focused on areas MT and on the dorsal portion of MST (MSTd) (e.g., de Jong et al. 1994; Smith and Scott-Samuel 1998; Morrone et al. 2000; Rutschmann et al. 2000; Ptito et al. 2001; Wunderlich et al. 2002; Smith et al. 2006). Figures often show only lateral views of the brain, sometimes making it difficult to assess whether the POS was also involved. The few studies that have reported involvement of the POS or precuneus for this kind of stimulation (e.g., Cheng et al. 1995; Brandt et al. 1998; Previc et al. 2000; Sereno et al. 2001; Kleinschmidt et al. 2002; Kovács et al. 2008) have not related it to the recently defined human V6.

Like neurons in MSTd, V6 neurons are direction- and speed-selective, both respond well to large stimuli (Eifuku and Wurtz 1998; Galletti et al. 1999), and both receive strong direct V1 input (Boussaoud et al. 1990; Sousa et al. 1991; Palmer and Rosa 2006). These 2 areas are also directly interconnected (Galletti et al. 2001). Given our results, it would be interesting to determine to what extent V6 neurons are selective to flow field parameters of the sort that have been extensively manipulated in the study of MSTd neurons in macaque (Saito et al. 1986; Tanaka et al. 1989; Duffy and Wurtz 1991a, 1991b; Orban et al. 1992; Graziano et al. 1994; Duffy 1998; Eifuku and Wurtz 1998; Paolini et al. 2000) and human (e.g., de Jong et al. 1994; Dupont et al. 1997; Smith and Scott-Samuel 1998; Morrone et al. 2000; Rutschmann et al. 2000; Ptito et al. 2001; Wunderlich et al. 2002; Smith et al. 2006). Given that receptive fields are slightly smaller in V6 than in MSTd, V6 may sit at a slightly earlier processing stage than MSTd and perhaps provides estimates of local translation to MSTd as suggested by several models (e.g., Sereno and Sereno 1991; Zhang et al. 1993). Our results suggest that V6 inputs may be more selective for locally coherent motion than MT is. Finally, it is important not to ignore V6′s other outputs to multimodal areas that coordinate visual, somatosensory, and motor information for reaching (V6A) and control and protection of the face and head (VIP).

Although human brain research has often drawn inspiration from results in nonhuman primate research, this is a 2-way street; the discovery of flow field sensitivity in human V6 will likely stimulate other laboratories to test for flow field sensitivity in macaque V6 using stimuli similar to those described here.

A Functional Localizer for Human V6

The most effective visual stimulus in driving human V6 across 4 different visual stimuli was Flow Fields. This stimulus is a good functional localizer for 3 reasons: First, V6 was always activated in response to this stimulus (100% of cases). The activation almost perfectly matched the location and limits of area V6 as previously defined in retinotopic mapping experiment. The focus of activation was selective and segregated from the activation of neighboring visual areas, in contrast to some localizers that also activate surrounding areas (e.g., motion vs. stationary activated areas beyond MT). This makes it possible for another laboratory to unambiguously find the borders of V6 without retinotopic mapping. Second, the selectivity of fMRI activation resulting from Flow Fields is consistent at the group level (Fig. 6). This increases its potential use given that many fMRI laboratories follow standard group protocols instead of individual subject analysis approach. Third, the Flow Fields stimulus can functionally localize area V6 even when a standard, nonwide stimulus is used. Wide-field stimulation is difficult to implement and few have done so (Pitzalis et al. 2006; Sereno and Huang 2006; Stenbacka and Vanni 2007); the ability to localize V6 with a standard size stimulus will broaden its application given that a majority of current fMRI laboratories display visual stimuli on standard back-projections screens extending at most to 10- to 15-deg eccentricity in visual field.

Finally, the third point above—that coherent optical flow outlines V6 with a standard-sized stimulus despite the fact that retinotopy requires wide-field stimulus—warrants a comment. It is important to keep in mind that phase-encoded retinotopic mapping has a lower sensitivity per unit time than 2-condition paradigms because retinotopic stimuli effectively divide the data from each run into many more bins (polar angles) than a 2-condition experiment does. Given the high sensitivity of V6 to coherent motion, peripheral receptive fields whose center is outside the edge of the stimulus field will likely have responded anyway; by contrast, the much more slowly moving retinotopic mapping stimuli are probably not optimal for stimulating V6 receptive fields. Future experiments using phase-encoded analogues of Flow Fields may be able to resolve this apparent paradox.

V5 and V6: 2 Motion Areas in the Dorsal Stream of the Human Brain

Present results demonstrate the existence in the human dorsal visual stream of a motion-sensitive area (V6) distinct from the classic motion-sensitive area MT+. As shown in Figure 9 (see also Fig. 6), the 2 motion areas are located in quite separate parts of the brain. The 2 areas are both activated by the moving stimuli in Drifting Edges (Fig. 4) and by the flickering stimulation (Fig. 7). However, a clear functional dissociation was found with more complex visual stimulations (see Fig. 5). In particular, MT+ is well activated by Radial Rings but not by Flow Fields and, conversely, area V6 is well activated by Flow

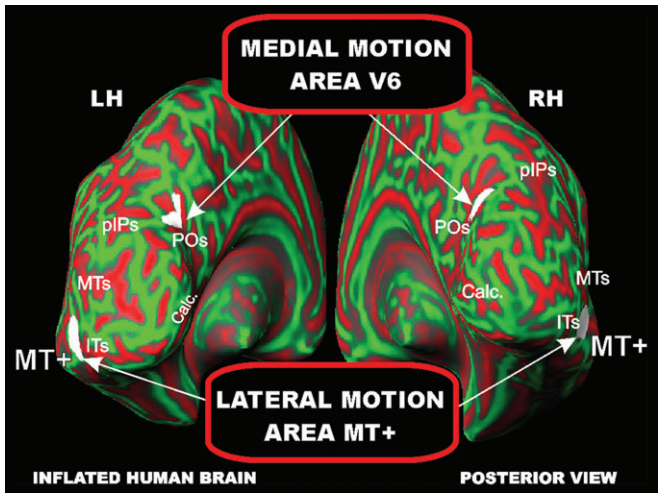

Figure 9. Brain location of the two motion areas V6 and MT+. Group fMRI activations for the Flow Fields and Radial Rings stimuli superimposed on the left and right inflated hemispheres (posterior view) of the SPM canonical brain in MNI space. Calc, Calcarine. Other labels and logos are as in Figures 4 and 6.

Fields but not by Radial Rings. This result suggests that the 2 dorsal motion areas perform different functions.

The present results suggest that MT+ encodes visual motion but does not strongly distinguish between coherent and incoherent motion. Note that single unit studies have shown some cross-direction inhibition in MT; we predict cross-direction inhibition should be much stronger in V6. This view is in line with previous neuroimaging studies showing no responses in area MT+ for coherent motion when incoherent motion was subtracted (e.g., McKeefry et al. 1997; Brandt et al. 1998; Previc et al. 2000; Rutschmann et al. 2000; Ptito et al. 2001; Beer et al. 2002) and with studies showing that medial occipital cortex is activated by coherent motion (e.g., Brandt et al. 1998; Previc et al. 2000; Sereno et al. 2001; Kleinschmidt et al. 2002).

It has been suggested (Previc 1998; Previc et al. 2000; Rosa and Tweedale 2001) that a lateral and a medial motion area (roughly MT+ and V6) are engaged in the detection of object motion and self-motion, respectively, and that the outputs of both of these areas converge on V6A (Shipp et al. 1998; Galletti et al. 2001) to help direct arm movements toward objects in extrapersonal space (see for review Rosa and Tweedale 2001; Galletti and Fattori 2003).

In the macaque, it has been suggested that area V6 is also involved in object-motion recognition (Galletti and Fattori 2003). The hypothesis is based on the fact that V6 contains many "real-motion cells," that is, cells activated by the actual movement of an object in the visual field, regardless of the movement of object retinal image induced by the eye movements. The evidence that V6 cells are sensitive to large visual stimuli, in particular to moving elongated luminance borders moving in constant directions, could help in understanding the meaning in term of direction of ego motion of the visual feedback evoked by translational ego motion (motion of the subject on a car, for instance, but even the visual stimulation evoked by head rotation). Even though area V6, and in particular those cells activated by elongated moving luminance borders, is not directly involved in the control of arm movement, we claim that V6 cells are able to recognize the event "real movement" in the visual field and to encode the direction of movement of objects in the visual field: These features could be useful for encoding the continuously changing spatial coordinates of moving objects that could be targets of reaching movements.

According to Galletti and Fattori (2003), MT/V5 would be involved in the analysis of motion signals (direction and speed of movement) particularly in the central part of the visual field, whereas V6 could also be involved in "subtracting out" self-motion across the whole visual field. The fact that the representation of the periphery in V6 is more emphasized in comparison with that in area MT/V5 (Gattass and Gross 1981; Galletti et al. 1999; Pitzalis et al. 2006) lends support to this view. Future studies playing off central and peripheral cues to self-motion and object motion will be needed to verify these hypotheses.

Funding

The Italian Ministry of Health (grants to The Neuroimaging Laboratory at Santa Lucia Foundation), the Italian Ministry of University and Research and Fondazione del Monte di Bologna e Ravenna, Italy (support for this work).

Notes

We are grateful to S. Sdoia and A. Stella for help with data analysis. We thank Anders Dale for writing the original IRIX GL version of the structured motion stimulus graphics code—it was originally designed to isolate MSTd—and Roger Tootell and John Reppas for helping us collect the first fMRI data using it. *Conflict of Interest*: None declared.

Address correspondence to Sabrina Pitzalis, Department of Education in Sport and Human Movement, University of Rome "Foro Italico," 00194 Rome, Italy. Email: sabrina.pitzalis@iusm.it.

References

Albright TD. 1984. Direction and orientation selectivity of neurons in visual area MT of the macaque. J Neurophysiol. 52(6): 1106–1130.

Allman JM, Kaas J. 1971. A representation of the visual field in the caudal third of the middle temporal gyrus of the owl monkey (*Aotus trivirgatus*). Brain Res. 31:85–105.

Allman JM, Kaas J. 1976. Representation of the visual field on the medial wall of the occipital–parietal cortex in the owl monkey. Science. 191:572–575.

Beer J, Blakemore C, Previc FH, Liotti M. 2002. Areas of the human brain activated by ambient visual motion, indicating three kinds of self-movement. Exp Brain Res. 143(1):78–88.

Blanke O, Landis T, Mermoud C, Spinelli L, Safran AB. 2003. Direction-selective motion blindness after unilateral posterior brain damage. Eur J Neurosci. 18(3):709–722.

Boussaoud D, Ungerleider LG, Desimone R. 1990. Pathways for motion analysis: cortical connections of the medial superior temporal and fundus of the superior temporal visual areas in the macaque. J Comp Neurol. 296(3):462–495.

Brandt T, Bucher SF, Seelos KC, Dieterich M. 1998. Bilateral functional MRI activation of the basal ganglia and middle temporal/medial superior temporal motion-sensitive areas: optokinetic stimulation in homonymous hemianopia. Arch Neurol. 55(8):1126–1131.

Brewer AA, Press WA, Logothetis NK, Wandell BA. 2002. Visual areas in macaque cortex measured using functional magnetic resonance imaging. J Neurosci. 22:10416–10426.

Cheng K, Fujita H, Kanno I, Miura S, Tanaka K. 1995. Human cortical regions activated by wide-field visual motion: an H2 150 PET study. J Neurophysiol. 74:413–427.

Dale AM, Fischl B, Sereno MI. 1999. Cortical surface-based analysis. I. Segmentation and surface reconstruction. Neuroimage. 9:179–194.

de Jong BM, Shipp S, Skidmore B, Frackowiak RS, Zeki S. 1994. The cerebral activity related to the visual perception of forward motion in depth. Brain. 117:1039–1054.

Dechent P, Frahm J. 2003. Characterization of the human visual V6 complex by functional magnetic resonance imaging. Eur J Neurosci. 17:2201–2211.

Desimone R, Ungerleider LG. 1986. Multiple visual areas in the caudal superior temporal sulcus of the macaque. J Comp Neurol. 248:164–189.

DeYoe EA, Bandettini P, Neitz J, Miller D, Winans P. 1994. Functional magnetic resonance imaging (FMRI) of the human brain. J Neurosci Methods. 54(2):171–187.

DeYoe EA, Carman GJ, Bandettini P, Glickman S, Wieser J, Cox R, Miller D, Neitz J. 1996. Mapping striate and extrastriate visual areas in human cerebral cortex. Proc Natl Acad Sci USA. 93:2382–2386.

Duffy CJ. 1998. MST neurons respond to optic flow and translational movement. J Neurophysiol. 80(4):1816–1827.

Duffy CJ, Wurtz RH. 1991a. Sensitivity of MST neurons to optic flow stimuli. I. A continuum of response selectivity to large-field stimuli. J Neurophysiol. 65(6):1329–1345.

Duffy CJ, Wurtz RH. 1991b. Sensitivity of MST neurons to optic flow stimuli. II. Mechanisms of response selectivity revealed by small-field stimuli. J Neurophysiol. 65(6):1346–1359.

Dupont P, De Bruyn B, Vandenberghe R, Rosier AM, Michiels J, Marchal G, Mortelmans L, Orban GA. 1997. The kinetic occipital region in human visual cortex. Cereb Cortex. 7(3):283–292.

Dupont P, Orban GA, De Bruyn B, Verbruggen A, Mortelmans L. 1994. Many areas in the human brain respond to visual motion. J Neurophysiol. 72(3):1420–1424.

Eifuku S, Wurtz RH. 1998. Response to motion in extrastriate area MSTl: center-surround interactions. J Neurophysiol. 80(1): 282–296.
Engel SA, Glover GH, Wandell BA. 1997. Retinotopic organization in human visual cortex and the spatial precision of functional MRI. Cereb Cortex. 7(2):181–192.
Engel SA, Rumelhart DE, Wandell BA, Lee AT, Glover GH, Chichilnisky EJ, Shadlen MN. 1994. fMRI of human visual cortex. Nature. 369(6481):525.
Felleman DJ, Kaas JH. 1984. Receptive-field properties of neurons in middle temporal visual area (MT) of owl monkeys. J Neurophysiol. 52(3):488–513.
Fischl B, Sereno MI, Dale AM. 1999. Cortical surface-based analysis. II: inflation, flattening, and a surface-based coordinate system. NeuroImage. 9:195–207.
Friston KJ, Ashburner J, Poline JB, Frith CD, Heather JD, Frackowiak RSJ. 1995. Spatial registration and normalization of images. Hum Brain Mapp. 2:165–189.
Friston KJ, Holmes A, Poline JB, Price CJ, Frith CD. 1996. Detecting activations in PET and fMRI: levels of inference and power. NeuroImage. 4:23–235.
Galati G, Pappata S, Pantano P, Lenzi GL, Samson Y, Pizzamiglio L. 1999. Cortical control of optokinetic nystagmus in humans: a positron emission tomography study. Exp Brain Res. 126(2):149–159.
Galletti C, Battaglini PP, Fattori P. 1991. Functional properties of neurons in the anterior bank of the parieto-occipital sulcus of the macaque monkey. Eur J Neurosci. 3:452–461.
Galletti C, Fattori P. 2003. Neuronal mechanisms for detection of motion in the field of view. Neuropsychologia. 41:1717–1727.
Galletti C, Fattori P, Battaglini PP, Shipp S, Zeki S. 1996. Functional demarcation of a border between areas V6 and V6A in the superior parietal gyrus of the macaque monkey. Eur J Neurosci. 8:30–52.
Galletti C, Fattori P, Gamberini M, Kutz DF. 1999. The cortical visual area V6: brain location and visual topography. Eur J Neurosci. 11: 3922–3936.
Galletti C, Gamberini M, Kutz DF, Fattori P, Luppino G, Matelli M. 2001. The cortical connections of area V6: an occipito-parietal network processing visual information. Eur J Neurosci. 13:1572–1588.
Gattass R, Gross CG. 1981. Visual topography of striate projection zone (MT) in posterior superior temporal sulcus of the macaque. J Neurophysiol. 46:621–638.
Gattass R, Sousa APB, Gross CG. 1988. Visuotopic organization and extent of V3 and V4 of the macaque. J Neurosci. 8:1831–1845.
Georgieva SS, Todd JT, Peeters R, Orban GA. 2008. The extraction of 3D shape from texture and shading in the human brain. Cereb Cortex. 18(10):2416–2438.
Graziano MS, Andersen RA, Snowden RJ. 1994. Tuning of MST neurons to spiral motions. J Neurosci. 14(1):54–67.
Hadjikhani N, Liu AK, Dale AM, Cavanagh P, Tootell RBH. 1998. Retinotopy and color sensitivity in human visual cortical area V8. Nature Neuroscience. 1:235–241.
Hagler DJ, Jr, Sereno MI. 2006. Spatial maps in frontal and prefrontal cortex. Neuroimage. 29:567–577.
Heide W, Koenig E, Dichgans J. 1990. Optokinetic nystagmus, self-motion sensation and their aftereffects in patients with occipito-parietal lesions. Clin Vis Sci. 5:145–156.
Huk AC, Dougherty RF, Heeger DJ. 2002. Retinotopy and functional subdivision of human areas MT and MST. J Neurosci. 22:7195–7205.
Kaas JH, Morel A. 1993. Connections of visual areas of the upper temporal lobe of owl monkeys: the MT crescent and dorsal and ventral subdivisions of FST. J Neurosci. 13(2):534–546.
Kleinschmidt A, Thilo KV, Büchel C, Gresty MA, Bronstein AM, Frackowiak RS. 2002. Neural correlates of visual-motion perception as object- or self-motion. Neuroimage. 16(4):873–882.
Koenderink JJ. 1986. Optic flow. Vision Res. 26:161–168.
Kovács G, Raabe M, Greenlee MW. 2008. Neural correlates of visually induced self-motion illusion in depth. Cereb Cortex. 18:1779–1787.
Lagae L, Maes H, Raiguel S, Xiao D-K, Orban GA. 1994. Responses of macaque STS neurons to optic flow components: a comparison of areas MT and MST. J Neurophysiol. 71:1597–1626.
Larsson J, Heeger DJ. 2006. Two retinotopic visual areas in human lateral occipital cortex. J Neurosci. 26(51):13128–13142.
Malonek D, Tootell RB, Grinvald A. 1994. Optical imaging reveals the functional architecture of neurons processing shape and motion in owl monkey area MT. Proc Biol Sci. 258(1352):109–119.
Maunsell JHR, Van Essen DC. 1983. Functional properties of neurons in the middle temporal visual area of the macaque monkey. I. Selectivity for stimulus direction, speed and orientation. J Neurophysiol. 49: 1127–1147.
Mazziotta JC, Toga AW, Evans A, Fox P, Lancaster J. 1995. A probabilistic atlas of the human brain: theory and rationale for its development. The International Consortium for Brain Mapping (ICBM). NeuroImage. 2:89–101.
McKeefry DJ, Watson JD, Frackowiak RS, Fong K, Zeki S. 1997. The activity in human areas V1/V2, V3, and V5 during the perception of coherent and incoherent motion. Neuroimage. 5(1):1–12.
Morrone MC, Tosetti M, Montanaro D, Fiorentini A, Cioni G, Burr DC. 2000. A cortical area that responds specifically to optic flow, revealed by fMRI. Nat Neurosci. 3:1322–1328.
Orban GA, Lagae L, Verri A, Raiguel S, Xiao D, Maes H, Torre V. 1992. First-order analysis of optical flow in monkey brain. Proc Natl Acad Sci USA. 89(7):2595–2599.
Palmer SM, Rosa MG. 2006. A distinct anatomical network of cortical areas for analysis of motion in far peripheral vision. Eur J Neurosci. 24(8):2389–405.
Paolini M, Distler C, Bremmer F, Lappe M, Hoffmann KP. 2000. Responses to continuously changing optic flow in area MST. J Neurophysiol. 84(2):730–743.
Pitzalis S, Galletti C, Huang RS, Patria F, Committeri G, Galati G, Fattori P, Sereno MI. 2006. Wide-field retinotopy defines human cortical visual area V6. J Neurosci. 26:7962–7973.
Portin K, Hari R. 1999. Human parieto-occipital visual cortex: lack of retinotopy and foveal magnification. Proc R Soc Lond B. 266:981–985.
Portin K, Vanni S, Virsu V, Hari R. 1999. Stronger occipital cortical activation to lower than upper visual field stimuli. Neuromagnetic recordings. Exp Brain Res. 124(3):287–294.
Previc FH. 1998. The neuropsychology of 3-D space. Psychol Bull. 124(2):123–164.
Previc FH, Liotti M, Blakemore C, Beer J, Fox P. 2000. Functional imaging of brain areas involved in the processing of coherent and incoherent wide field-of-view visual motion. Exp Brain Res. 131(4): 393–405.
Ptito M, Kupers R, Faubert J, Gjedde A. 2001. Cortical representation of inward and outward radial motion in man. Neuroimage. 14(6): 1409–1415.
Richer F, Martinez M, Cohen H, Saint-Hilaire JM. 1991. Visual motion perception from stimulation of the human medial parieto-occipital cortex. Exp Brain Res. 87:649–652.
Rodman HR, Albright TD. 1989. Single-unit analysis of pattern-motion selective properties in the middle temporal visual area (MT). Exp Brain Res. 75(1):53–64.
Rosa MG, Elston GN. 1998. Visuotopic organisation and neuronal response selectivity for direction of motion in visual areas of the caudal temporal lobe of the marmoset monkey (*Callithrix jacchus*): middle temporal area, middle temporal crescent, and surrounding cortex. J Comp Neurol. 393(4):505–27.
Rosa MG, Tweedale R. 2001. The dorsomedial visual areas in New World and Old World monkeys: homology and function. Eur J Neurosci. 13(3):421–427.
Rutschmann RM, Schrauf M, Greenlee MW. 2000. Brain activation during dichoptic presentation of optic flow stimuli. Exp Brain Res. 134(4):533–537.
Saito H, Yukie M, Tanaka K, Hikosaka K, Fukada Y, Iwai E. 1986. Integration of direction signals of image motion in the superior temporal sulcus of the macaque monkey. J Neurosci. 6(1):145–157.
Sereno MI. 1998. Brain mapping in animals and humans. Curr Opin Neurobiol. 8:188–194.
Sereno MI, Dale AM, Reppas JB, Kwong KK, Belliveau JW, Brady TJ, Rosen BR, Tootell RB. 1995. Borders of multiple visual areas in humans revealed by functional magnetic resonance imaging. Science. 268: 889–893.

Sereno MI, Huang RS. 2006. A human parietal face area contains aligned head-centered visual and tactile maps. Nat Neurosci. 9(10):1337–1343.
Sereno MI, McDonald CT, Allman JM. 1994. Analysis of retinotopic maps in extrastriate cortex. Cereb Cortex. 4:601–620.
Sereno MI, Pitzalis S, Martínez A. 2001. Mapping of contralateral space in retinotopic coordinates by a parietal cortical area in humans. Science. 294:1350–1354.
Sereno MI, Sereno ME. 1991. Learning to see rotation and dilation with a Hebb rule. In: Lippmann RP, Moody JE, Touretzky DS, editors. Advances in neural information processing systems 3. San Mateo (CA): Morgan Kaufmann Publishers. p. 320–326.
Sereno MI, Tootell RBH. 2005. From monkeys to humans: what do we now know about brain homologies? Curr Opin Neurobiol. 15:135–144.
Shipp S, Blanton M, Zeki S. 1998. A visuo-somatomotor pathway through superior parietal cortex in the macaque monkey: cortical connections of areas V6 and V6A. Eur J Neurosci. 10(10):3171–3193.
Shipp S, Zeki S. 1989. The Organization of connections between areas V5 and V1 in macaque monkey visual cortex. Eur J Neurosci. 1(4):309–332.
Siegel RM, Read HL. 1997. Analysis of optic flow in the monkey parietal area 7a. Cereb Cortex. 7(4):327–346.
Smith AT, Greenlee MW, Singh KD, Kraemer FM, Hennig J. 1998. The processing of first- and second-order motion in human visual cortex assessed by functional magnetic resonance imaging (fMRI). J Neurosci. 18:3816–3830.
Smith AT, Scott-Samuel NE. 1998. Stereoscopic and contrast-defined motion in human vision. Proc Biol Sci. 265(1405):1573–1581.
Smith T, Wall MB, Williams AL, Singh KD. 2006. Sensitivity to optic flow in human cortical areas MT and MST. Eur J Neurosci. 23:561–569.
Sousa AP, Piñon MC, Gattass R, Rosa MG. 1991. Topographic organization of cortical input to striate cortex in the Cebus monkey: a fluorescent tracer study. J Comp Neurol. 308(4):665–682.
Stenbacka L, Vanni S. 2006. Central luminance flicker can activate peripheral retinotopic representation. NeuroImage. 34:342–348.
Stenbacka L, Vanni S. 2007. fMRI of peripheral visual field. Clin Neurophysiol. 118:1303–1314.
Tanaka K, Fukada Y, Saito HA. 1989. Underlying mechanisms of the response specificity of expansion/contraction and rotation cells in the dorsal part of the medial superior temporal area of the macaque monkey. J Neurophysiol. 62(3):642–656.
Tootell RB, Dale AM, Sereno MI, Malach R. 1996. New images from human visual cortex. Trends Neurosci. 19(11):481–489Review.
Tootell RB, Hadjikhani N. 2001. Where is 'dorsal V4' in human visual cortex? Retinotopic, topographic and functional evidence. Cereb Cortex. 11:298–311.
Tootell RB, Hadjikhani N, Hall EK, Marrett S, Vanduffel W, Vaughan JT, Dale AM. 1998. The retinotopy of visual spatial attention. Neuron. 21:1409–1422.
Tootell RB, Mendola JD, Hadjikhani NK, Ledden PJ, Liu AK, Reppas JB, Sereno MI, Dale AM. 1997. Functional analysis of V3A and related areas in human visual cortex. J Neurosci. 17:7076–7078.
Tootell RB, Reppas JB, Kwong KK, Malach R, Born RT, Brady TJ, Rosen BR, Belliveau JW. 1995. Functional analysis of human MT and related visual cortical areas using magnetic resonance imaging. J Neurosci. 15:3215–3230.
Van Essen DC, Maunsell HR, Bixby JL. 1981. The middle temporal visual area in the macaque: myeloarchitecture, connections, functional properties and topographic organization. J Comp Neurol. 199: 293–326.
Van Oostende S, Sunaert S, Van Hecke P, Marchal G, Orban GA. 1997. The kinetic occipital (KO) region in man: an fMRI study. Cereb Cortex. 7:690–701.
Vanni S, Tanskanen T, Seppa M, Uutela K, Hari R. 2001. Coinciding early activation of the human primary visual cortex and anteromedial cuneus. Proc Natl Acad Sci USA. 98(5):2776–2780.
Vogt-Weisenhorn DM, Illing RB, Spatz WB. 1995. Morphology and connections of neurons in area 17 projecting to the extrastriate areas MT and 19DM and to the superior colliculus in the monkey *Callithrix jacchus*. J Comp Neurol. 362(2):233–55.
Wandell BA, Brewer AA, Dougherty RF. 2005. Visual field map clusters in human cortex. Philos Trans R Soc Lond B Biol Sci. 360: 693–707.
Watson JD, Myers R, Frackowiak RS, Hajnal JV, Woods RP, Mazziotta JC, Shipp S, Zeki S. 1993. Area V5 of the human brain: evidence from a combined study using positron emission tomography and magnetic resonance imaging. Cereb Cortex. 3:79–94.
Wiest G, Zimprich F, Prayer D, Czech T, Serles W, Baumgartner C. 2004. Vestibular processing in human paramedian precuneus as shown by electrical cortical stimulation. Neurology. 62:473.
Worsley KJ, Evans AC, Marrett S, Neelin P. 1992. A three-dimensional statistical analysis for rCBF activation studies in human brain. J Cereb Blood Flow Metab. 12:900–918.
Wunderlich G, Marshall JC, Amunts K, Weiss PH, Mohlberg H, Zafiris O, Zilles K, Fink GR. 2002. The importance of seeing it coming: a functional magnetic resonance imaging study of motion-in-depth towards the human observer. Neuroscience. 112(3): 535–540.
Zarahn E, Aguirre GK, D'Esposito M. 1997. Empirical analyses of BOLD fMRI statistics. I. Spatially unsmoothed data collected under null-hypothesis conditions. Neuroimage. 5:179–197.
Zeki S. 1980. The response properties of cells in the middle temporal area (area MT) of owl monkey visual cortex. Proc R Soc Lond B Biol Sci. 207(1167):239–248.
Zeki S, Watson JDG, Lueck CJ, Friston KJ, Kennard C, Frackowiak RSJ. 1991. A direct demonstration of functional specialization in the human visual cortex. J Neurosci. 11:641–649.
Zeki SM. 1974. Functional organization of a visual area in the posterior bank of the superior temporal sulcus of the rhesus monkey. J Physiol (Lond.). 236:549–573.
Zhang KE, Sereno MI, Sereno ME. 1993. Emergence of position-independent detectors of sense of rotation and dilation with Hebbian learning: an analysis. Neural Comput. 5:597–612.